Attention-based Multi-Context Guiding for Few-Shot Semantic Segmentation

Tao Hu[1,2],Pengwan Yang[2], Chiliang Zhang[3], Gang Yu[4], Yadong Mu[2], Cees G. M. Snoek[1]

[1]University of Amsterdam, the Netherlands
[2]Peking University, China
[3]Tsinghua University, China
[4]Megvii Inc. (Face++), China

taohu620@gmail.com,yangpengwan2016@gmail.com,zhangcl16@mails.tsinghua.edu.cn
yugang@megvii.com,myd@pku.edu.cn,cgmsnoek@uva.nl

Abstract

Few-shot learning is a nascent research topic, motivated by the fact that traditional deep learning methods require tremendous amounts of data. The scarcity of annotated data becomes even more challenging in semantic segmentation since pixel-level annotation in segmentation task is more labor-intensive to acquire. To tackle this issue, we propose an Attention-based Multi-Context Guiding (A-MCG) network, which consists of three branches: the support branch, the query branch, the feature fusion branch. A key differentiator of A-MCG is the integration of multi-scale context features between support and query branches, enforcing a better guidance from the support set. In addition, we also adopt a spatial attention along the fusion branch to highlight context information from several scales, enhancing self-supervision in one-shot learning. To address the fusion problem in multi-shot learning, Conv-LSTM is adopted to collaboratively integrate the sequential support features to elevate the final accuracy. Our architecture obtains state-of-the-art on unseen classes in a variant of PASCAL VOC12 dataset and performs favorably against previous work with large gains of 1.1%, 1.4% measured in mIoU in the 1-shot and 5-shot setting.

Introduction

The state-of-the-art in image classification, detection and segmentation have been greatly advanced by convolution neural networks (CNN). Although CNNs exhibit superior performances in a variety of tasks, it has the key problem of being data hungry. Typically gigantic data with annotations are required for achieving high accuracy. This issue becomes more severe for pixel-level annotations. In recent years, there emerged a new research thrust which learns new concepts from limited data, known as few-shot learning (Vinyals et al. 2016; Snell, Swersky, and Zemel 2017; Ravi and Larochelle 2017). Though widely explored in tasks like image classification, few-shot learning is rarely considered for dense pixel prediction problems.

Most existing methods in few-shot semantic segmentation are based on the framework shown in the top panel of Fig. 1. Conceptually, the framework is comprised of a support branch and a query branch. The support branch provides discriminative support feature to assist the target segmentation,
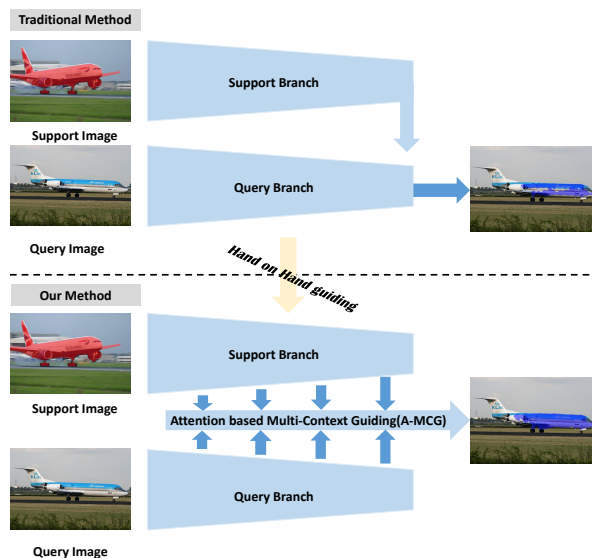
Figure 1: Our motivation. The support image mask is overlaid with ground truth in red, the query image is overlaid with ground truth in blue. The above is previous method, the below is our method. Our A-MCG network can help the support branch fuse multi-context information to hand on hand guide the query branch.

the query branch is the feature extractor for target segmentation. This paradigm has the following difficulties: (1). *Inefficient support feature utilization.* The feature of the support branch is precious, as it determines the final category the network will segment. However, most of the previous methods only consider the single output from the end of the network, which do not take full advantage of the multi-context feature. (2). *Lack of attention.* As the amount of support and query data is often very small, optimization based on a large amount of data is impossible, some self-supervised methods such as attention should be introduced to make the network concentrate on our target class. (3). *Inconvenience in multi-shot learning.* The traditional fusion method for multi-shot semantic segmentation is the logical or operation, this inflexible approach lacks in exploring the inner common feature between various support images.

To attack the above problems in few-shot semantic segmentation, we propose an Attention-based Multi-Context Guiding network (A-MCG) shown in the bottom of Fig. 1. Our A-MCG tries to fuse small-to-large scale context information to globally guide the query branch to make the right segmentation decision. A multi-context feature will largely facilitate the query branch segmentation based on multiple scales of support feature. In addition, we utilize the Residual Attention Module(RAM) (Wang et al. 2017) to carry out a self-supervised attention for further improvement of the segmentation. To deal with multi-shot learning, Conv-LSTM (Xingjian et al. 2015) is incorporated for better fusing multi-shot support feature.

Our A-MCG network makes the following contributions: (1). We first propose a Multi-Context Guiding structure to fuse the small-to-large scale context features between support branch and query branch to globally guide the query branch segmentation. (2). We introduce a Residual Attention Module (Wang et al. 2017) in our MCG network to realize the attention mechanism in few-shot learning of segmentation. (3). We embed the Conv-LSTM (Xingjian et al. 2015) module into the end of our network to better merge the feature map from support set in multi-shot semantic segmentation. (4). Compared with previous methods, our A-MCG reaches state-of-the-art 61.2%, 62.2% measured in mIoU in the 1-shot and 5-shot setting.

Related Work

Semantic Segmentation. During the early period, the CNN is only employed in the classification tasks, most of them (Krizhevsky, Sutskever, and Hinton 2012; Szegedy et al. 2015) are composed of convolution layers and fully connected layers. Fully Convolutional Network(FCN) (Long, Shelhamer, and Darrell 2015) first applies CNN for the task of image semantic segmentation. FCN's key contribution is building a "fully convolutional" network that takes an input of arbitrary size and produces correspondingly-sized output with efficient inference and learning.

In Deeplab (Chen et al. 2018), Dilated Convolutions are introduced as an alternative to CNN pooling layers in deep part to capture larger context without reducing the image resolution. A module named Atrous Spatial Pyramid Pooling (ASPP) is also included in Deeplab where parallel Dilated Convolution layers with different rates capture multi-scale information. Our method is also illuminated by the multi-context fusion pattern of ASPP and merges the multi-context information by borrowing the multi-scale context from the support branch and the query branch.

Attention Mechanism. In this paper, we mainly talk about two types of attention mechanism: (1). *Spatial Attention* such as Residual Attention Module(RAM) (Wang et al. 2017). Inside each Attention Module, an Hourglass-like (Newell, Yang, and Deng) bottom-up and top-down feedforward structure is used for generating attention map. (2). *Channel Attention* like SENet (Hu, Shen, and Sun 2018). "Squeeze-and-Excitation"(SE) block is designed that adaptively recalibrates channel-wise feature responses by explicitly modeling interdependencies between channels. We em-

Table 1: Problem Formulation Notations.

notation	meaning
I_S^i	i-th image in support set
$Y_S^i(l)$	i-th image-binary mask for class l
$S = \{(I_S^i, Y_S^i(l))\}_{i=1}^k$	support set
I_q	image in query set
L_{train}	train label set
L_{test}	test label set

ploy these two types of attention mechanism into our MCG architecture.

Few-Shot Learning in Semantic Segmentation. The first work in few-shot semantic segmentation is OSLSM (Shaban et al. 2017). They proposed the basic paradigm in few-shot segmentation. The support branch and the query branch are constructed by VGG (Simonyan and Zisserman 2014) to supervise training. However, the structure is not fully convolutional, which leads to inefficient utilization of spatial information. Later co-FCN (Rakelly et al. 2018) turns both of the support and query branches into FCN architecture, but the exploration of multi-scale context is not as thorough as our method.

On the other side, OSVOS (Caelles et al. 2017) tries to solve the task of semi-supervised video object segmentation. OSVOS is also based on a fully-convolutional network architecture and transfers generic semantic information to the task of foreground segmentation. OSVOS shows the effectiveness of fine-tuning for video object segmentation, but fine-tuning for every test video is too time-consuming.

Convolutional Long Short-Term Memory. Long Short-Term Memory(LSTM) (Hochreiter and Schmidhuber) is proposed as a special RNN structure to model long-range dependencies in various previous studies. However, LSTM is not suitable for handling spatiotemporal data because the input-to-state and state-to-state are all full connections thus no spatial information is encoded. To tackle this problem, Conv-LSTM (Xingjian et al. 2015) is put forward by using a convolution operator in the state-to-state and input-to-state transitions.

In our network, Conv-LSTM works as a memory unit to capture and integrate the previous support set feature for better multi-shot learning in semantic segmentation. Conv-LSTM's advantage is not only modeling the sequential data, but also sequentially filtering and fusing the data by gate mechanism. This method gives us more interpretability and can better smoothen our k-shot learning result compared with traditional fusion method.

Our Method

Problem Formulation

We follow the paradigm and notations in (Shaban et al. 2017), which are detailed in Table 1. The target is to learn a model $f(I_q, S)$ that, when given a support set S and query image I_q, predicts a binary mask $\hat{M}_q$ for the semantic class l. The f function is parameterized by neural networks of the
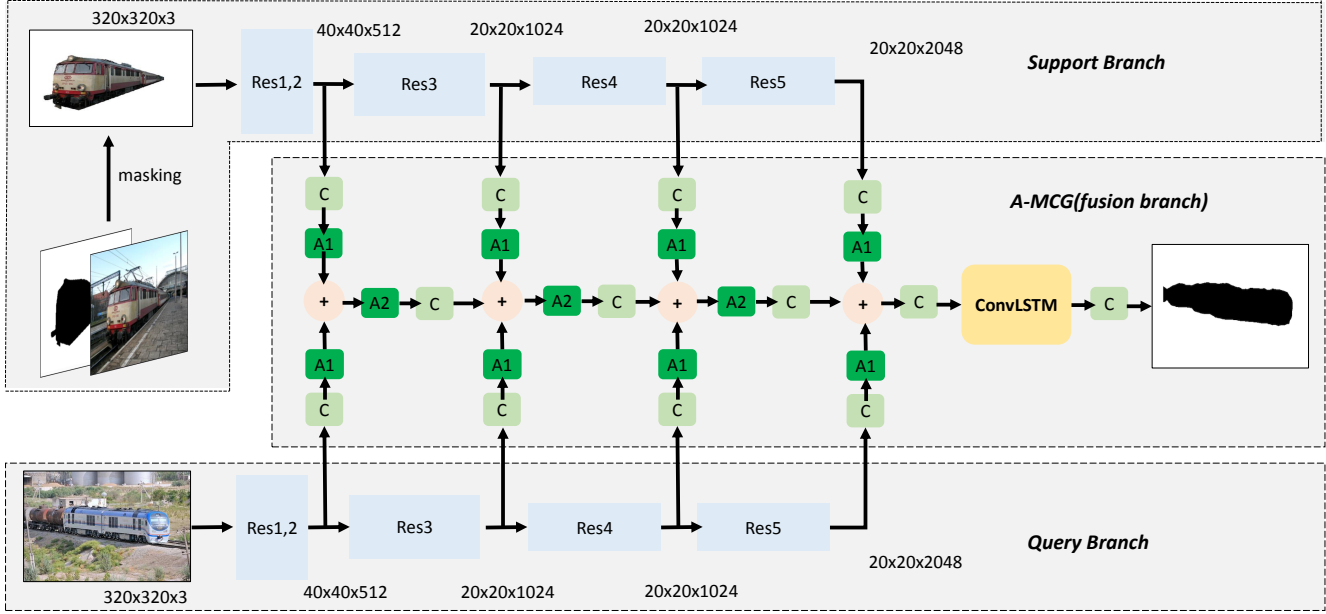
Figure 2: Attention-based Multi-Context Guiding Network Architecture for One-Shot Segmentation. It includes three parts: (1). the support branch. (2). the query branch. (3). A-MCG module. Res1, 2, 3, 4, 5 represent different block in ResNet. C is 1×1 convolution unit, stride=2 convolution is employed when the feature map size becomes smaller. We design two exclusive location settings of attention mechanism: A1, A2. The details of the attention architecture are illustrated in Fig. 4.

support branch and the query branch.

During training, the algorithm has access to a large set of image-mask pairs $D = \{(I^j, Y^j)\}_{j=1}^N$ where $Y^j \in L_{train}^{H \times W}$ is the binary mask for training image I^j. At testing, the query images are only annotated for new(unseen) semantic classes i.e. $L_{train} \cap L_{test} = \phi$, which leads us to divide the PASCAL VOC12 dataset like Table 2. This is the key difference between one-shot learning for segmentation and traditional segmentation, what we really care about is the segmentation performance on unseen data. Similar to the extension from one-shot learning to k-shot learning in classification task, k-shot learning can also be applied in semantic segmentation. In OSLSM (Shaban et al. 2017), k-shot learning results are fused by a logical OR operation between the k binary masks.

Attention Mechanism Review

Residual Attention Module(RAM) is first proposed by Wang *et al.* (Wang et al. 2017) for image classification. We here review the structure of RAM in Fig. 4. The original RAM proceeds many ablation studies for its setting, we directly use the explored optimal structure. In our paper, we mainly explore the attention location in our MCG module in Sec. Experimental Result.

The RAM actually utilizes a two-scale(down sample 2 times, then up sample 2 times) Hourglass structure to construct a soft attention mask M(x). In the original ResNet (He et al. 2016), residual learning is formulated as:

$$H_{i,c} = x + F_{i,c}(x) \tag{1}$$

where $F_{i,c}(x)$ approximates the residual function, i ranges over all spatial positions and $c \in \{1, ..., C\}$ is the index of the channel.

In RAM, the attention module is modified as:

$$H_{i,c} = (1 + M_{i,c}(x)) * F_{i,c}(x) \tag{2}$$

M(x) ranges from [0,1] because of the sigmoid function. With M(x) approximating 0, H(x) will approximate original features F(x). The key of RAM lies in M(x), which works as feature selectors that enhance good features and suppress noises from trunk features. This characteristic of RAM is particularly important for few-shot learning cases.

Except that, we also explored the SE block (Hu, Shen, and Sun 2018), which is a typical channel attention structure. Our later ablation study in Sec. Experimental Result shows that SE block fails to compete with RAM under the condition of same parameters.

Attention-based MCG

We propose an Attention-based Multi-Context Guiding network (A-MCG) illustrated in Fig. 2. Our A-MCG network is composed of three parts: (1). the support branch. (2). the query branch. (3). A-MCG(fusion) branch. The backbones of the support branch, the query branch are ResNet101. We elaborate our network as input image size 320×320, and their output feature map size is also marked in Fig. 2. Notably, the convolutions in Res-4, Res-5 blocks are equipped with Dilated Convolution (Chen et al. 2018) whose dilated rate=2. Therefore, the feature map size no long decreases

after Res-3, but the receptive field continues to be enlarged due to Dilated Convolution.

Our A-MCG module tries to utilize multi-context feature from the support branch to globally improve the query branch segmentation. We attempt two types of attention location pattern. In the following, we denote the b_s^i as feature maps after Res-i block in the support branch, b_q^i as feature maps after Res-i block in query branch, C as naive convolution(without ReLU (Nair and Hinton 2010), BN), H as our attention function, F_i as the mixed features after Res-i block of the support branch and the query branch.

Therefore, we mainly come up with three variants.

(1). Multi-context guiding module:

$$F_{i+1} = C\{C(b_s^i) + C(b_q^i) + F_i\} \qquad (3)$$

Multi-context information from both branches are mixed by convolution operation. Notably, convolution here doesn't include ReLU, BN.

(2). Multi-context guiding with separate attention:

$$F_{i+1} = C\{H(C(b_s^i)) + H(C(b_q^i)) + F_i\} \qquad (4)$$

which corresponds to A1 in Fig. 2.

Attention mechanism is employed separately both in the query branch and the support branch.

(3). Multi-context guiding with share attention:

$$F_{i+1} = C\{H(C(b_s^i) + C(b_q^i) + F_i)\} \qquad (5)$$

which corresponds to A2 in Fig. 2.

Attention mechanism is applied after the fusion of the query branch and the support branch.

Convolutional LSTM for k-shot learning

In previous work, we mainly focus on the circumstance of 1-shot learning in semantic segmentation. How shall we deal with k-shot learning? In OSLSM (Shaban et al. 2017), k-shot learning results are fused by a logical OR operation. However, this straightforward process is unexplainable and fails to utilize the inner relationship between sequential support images.

To better solve this multi-shot learning problem, we attempt to embed Conv-LSTM (Xingjian et al. 2015) at the end of the fusion branch as illustrated in Fig. 2. At last, a 1×1 convolution will be appended to generate segmentation probability map.

Conv-LSTM is first applied to the precipitation nowcasting task. The key idea of Conv-LSTM is to implement all operations, including state-to-state and input-to-state transitions, with kernel-based convolutions. The inner feature of the sequential support image mask can be sustained by Conv-LSTM. We here adopt a popular LSTM variant with "peephole connections" (Gers, Schraudolph, and Schmidhuber 2002). In detail, the three gating functions in Conv-LSTM are calculated according to the equations below:

$$i_t = \sigma(\boldsymbol{W}_{x,i} \otimes \boldsymbol{X}_t + \boldsymbol{W}_{h,i} \otimes \boldsymbol{H}_{t-1} + \boldsymbol{W}_{c,i} \otimes \boldsymbol{C}_{t-1}) \quad (6)$$

$$o_t = \sigma(\boldsymbol{W}_{x,o} \otimes \boldsymbol{X}_t + \boldsymbol{W}_{h,o} \otimes \boldsymbol{H}_{t-1} + \boldsymbol{W}_{c,o} \otimes \boldsymbol{C}_t) \quad (7)$$

$$f_t = \sigma(\boldsymbol{W}_{x,f} \otimes \boldsymbol{X}_t + \boldsymbol{W}_{h,f} \otimes \boldsymbol{H}_{t-1} + \boldsymbol{W}_{c,f} \otimes \boldsymbol{C}_{t-1}) \quad (8)$$
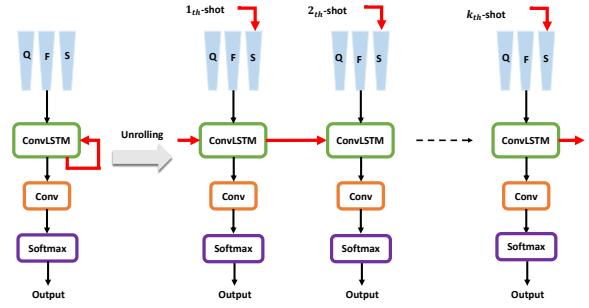

Figure 3: Unrolling view of Conv-LSTM. Q, F, S represents the query branch, the fusion branch, the support branch accordingly. Best viewed in color.

where we let $\boldsymbol{X}_t, \boldsymbol{H}_t$ be the input/hidden state at time t respectively. $\otimes$ represents spatio-temporal convolution operator.

Investigating previous $\boldsymbol{H}$ and current $\boldsymbol{X}$, the recurrent model synthesizes a new proposal for the cell state, namely

$$\tilde{C}_t = tanh(\boldsymbol{W}_{x,c} \otimes \boldsymbol{X}_t + \boldsymbol{W}_{h,c} \otimes \boldsymbol{H}_{t-1}) \qquad (9)$$

The final cell state is obtained by linearly fusing the new proposal $\tilde{C}_t$ and previous state $\boldsymbol{C}_{t-1}$:

$$\boldsymbol{C}_t = f_t \odot \boldsymbol{C}_{t-1} + i_t \odot \tilde{C}_t \qquad (10)$$

where $\odot$ denotes the Hadamard product. To continue the recurrent process, it also renders a filtered new H:

$$\boldsymbol{H}_t = o_t \odot tanh(\boldsymbol{C}_t) \qquad (11)$$

In our previous structure, the network is trained on one-shot support set. Once Conv-LSTM is imported into our framework, it will enable us to train with k-shot support set. For every batch(if batch size=1), one query image and k support image masks will be fed into our neural network.

We unroll this procedure in Fig. 3 for better understanding the k-shot fusion process. k-shot support image masks enter Conv-LSTM in turn. Conv-LSTM plays a critical role in summarizing the total features of the k-shot support image masks.

For better mixing the feature from the support set in k-shot learning, a function loss is designed as follows:

$$L = -\frac{1}{ks^2} \sum_{i=0}^{k} \sum_{m=0,n=0}^{s} Y_{m,n} log X_{m,n} \qquad (12)$$

where Y is binary label, X means the neural network output probability, k is shot number, s represents image size.

This loss enforces our A-MCG module to function well on **every** support set image rather than only supervises the segmentation of single support image.

Experimental Result

Training details

We implement our code based on the tensorflow framework (Abadi et al. 2016). Specially, a scaffold framework
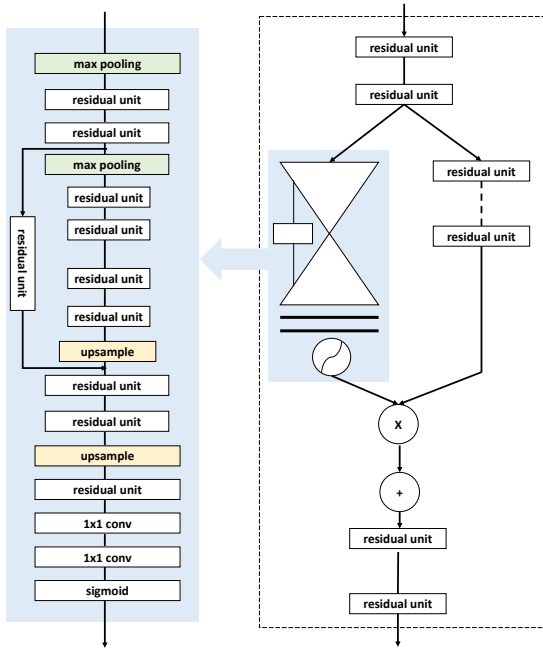
Figure 4: Residual Attention Module(RAM). Left side is an hourglass-like Soft Mask Branch, followed by a sigmoid operation. Right side is the whole structure of RAM. "residual unit" is a typical bottleneck structure which is detailed in ResNet (He et al. 2016).

named tensorpack (Wu and others 2016) is used for quickly setting up our experiment. All our models are trained by Stochastic Gradient Descent(SGD) (Bottou 2010) solver with learning rate=1e-4, momentum=0.99 on one Nvidia Titan XP GPU. To fully fill GPU memory, we set the batch size 12. The weights of the support branch and the query branch are initialized with ImageNet (Deng et al. 2009) pre-trained weights. For the weight initialization of A-MCG module, Xavier initialization (Glorot and Bengio 2010) is adopted. All the images in the support and query branch are resized to 320×320. No further augmentation is employed except the image resizing. For Batch Normalization(BN) (Ioffe and Szegedy 2015), we employ current batch statistics at training and use the moving average statistics of BN during validation time.

We use the cross-entropy loss as the object function for training the network. The loss is summed up over all the pixels in a mini-batch.

When we experiment with Conv-LSTM for k-shot learning, we set k=5 by default. The max batch size can only be 6 because every time k support image masks will be fed into the support branch. Layer Normalization (Ba, Kiros, and Hinton 2016) is utilized in our Conv-LSTM for speeding up convergence.

Dataset and Metric

Dataset: We utilize dataset PASCAL-5^i (Shaban et al. 2017) to conduct our experiment. This dataset is originated

Table 2: PASCAL-i^5 group information. The top table displays 4 groups of label and their semantic classes. The bottom table shows 4 sub-datasets and their training, validation components.

label set index	Semantic Classes
0	aeroplane, bicycle, bird, boat, bottle
1	bus, car, cat, chair, cow
2	diningtable, dog, horse, motorbike, person
3	potted plant, sheep, sofa, train, tv/monitor

sub-dataset	train label set	val label set
0	1,2,3	0
1	0,2,3	1
2	0,1,3	2
3	0,1,2	3

from PASCAL VOC12 (Everingham et al.) and extended annotations from SDS (Hariharan et al.). The set of 20 classes in PASCAL VOC12 is divided into four sub-datasets as indicated in Table 2. Three sub-datasets are used as the training label-set L_{train}, the left one sub-dataset is utilized for test label-set L_{test}.

The training set D_{train} is composed of all image-mask pairs from PASCAL VOC12 and SDS training sets that include at least one pixel in the segmentation mask from the label-set L_{train}. The masks in D_{train} are modified into binary masks by setting pixels whose semantic class are not in L_{train} as background class l_ϕ. The test set D_{test} is from PASCAL VOC12 and SDS validation sets, and the processing procedure for test set D_{test} is similar with training set D_{train}. Our evaluation mIoU is the average of 5 sub-dataset mIoUs. For a fair comparison with (Shaban et al. 2017), we take the same random seed and sample N=1000 examples for testing each of our models.

Metric: To compare the quantitative performance of the different models, mean intersection over union(mIoU) over two classes is used for our benchmark evaluation. For binary segmentation in our work, we first calculate the 2×2 confusion matrix, then compute the according IoU_l as $\frac{tp_l}{tp_l+fp_l+fn_l}$. tp_l is the number of true positives for class l, fp_l is the number of false positives for class l and fn_l is the number of false negatives for class l. The final mIoU is its average over the set of classes.

Ablation Study

Baseline. Our method is mostly compared with OSLSM (Shaban et al. 2017) and co-FCN (Rakelly et al. 2018). Both of them utilize the VGG (Simonyan and Zisserman 2014) as basic model. Different from them, we adopt ResNet101 (He et al. 2016) as our basic model, for ResNet101 owns much less parameter than VGG16, thus it is less prone to over-fitting. Besides, ResNet also enables larger batch size training in our architecture.

After removing the fully connected layers in the end, our

Table 3: Ablation Study for fusion width. The experiment is conducted on PASCAL-i^5 sub-dataset 0.

fusion width	1-shot	#params(M)
64	63.4	85.6
128	63.3	86.1
256	63.6	87.2
512	63.6	89.8
1024	63.2	96.1

Table 4: Ablation Study for multi-context pattern. The experiment is conducted on PASCAL-i^5 sub-dataset 0.

Method	1-shot	#params(M)
context-2345	63.6	87.2
context-45	63.2	86.7
context-5	61.2	86.1

ResNet101 baseline becomes a fully-convolutional structure. Support branch and query branch are fused by element-wise Add between the Res-5 output of them, followed by a naive convolution.

MCG: We explore several factors of our Multi-Context Guiding(MCG) architecture such as (1). *fusion width*. Fusion width is the channel number in the MCG branch, all the features in the support branch and the query branch will be transformed into features with width of fusion width. Different settings of fusion width are stated in Table 3. (2). *multi-context pattern*, we try to explore what kind of context combination is better for the few-shot learning in Table 4. The number after "context" is the feature we will adopt for fusion. For example, context-45 means that only features from Res-4, Res-5 are used for fusion. For convenience, we only proceed the ablation study in the sub-dataset 0 in this part.

From Table 3, we can conclude that when the fusion width is too small such as 64 ,128, the one-shot mIoU is 0.2% lower than width=256. Meanwhile, larger fusion width like 1024 will make the mIoU worse due to over-fitting. Taking into consideration of the balance between mIoU and parameter cost, we choose fusion width=256 as our default setting. The latter ablation study will also adopt the default value.

As for the multi-context pattern in Table 4, more level context fusion often leads to a better result. Context-2345 outperforms context-5 nearly 2.4% mIoU. This shows that our multi-context guiding strategy works as our motivation. Multi-context information fusion from both the support branch and the query branch could efficiently "support" the query branch's segmentation.

Attention Mechanism. We set two variants about the attention module: (1). *Spatial Attention*. Residual Attention Module(RAM) is applied here as a representative method. (2). *Channel Attention*. SENet (Hu, Shen, and Sun 2018) is explored in our ablation study. At the same time, two attention location patterns "separate" and "share" are also explored. "sep" denotes the support branch and query branch adopt separate attention. "share" represents the support
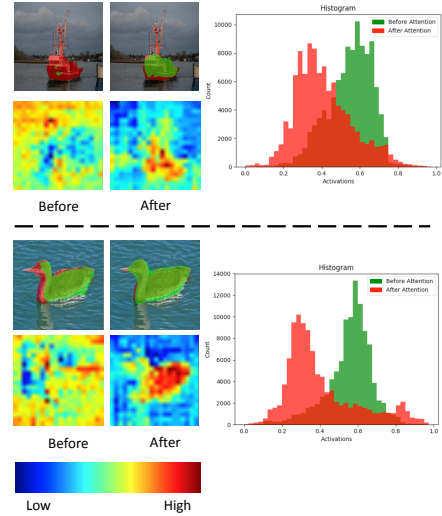

Figure 5: Attention Mechanism Visualization. Two images are demonstrated for the comparison between "before attention" and "after attention". The image is overlaid with predicted mask in green. The according histogram of the feature map is displayed in the right side. The feature map's activation value is normalized to 1. The support image is ignored. Best viewed in color.

branch and query branch share the same attention.

As shown in Table 5. We can find that Spatial Attention works much better than Channel Attention under the circumstance of same parameters. We conclude that spatial information is more useful in dense pixel task like image segmentation, while channel information plays a more important role in classification task.

It can be obviously figured out that sharing the same attention is basically better than separate attention. We speculate that for the support branch, the input has been already masked so that it does not need attention mechanism, while sharing attention mechanism will make the query branch pay more attention to the support branch's input mask.

On the other hand, we demonstrate some images' feature map visualization and feature map histogram in Fig. 5. From the visualization, we can qualitatively observe that the feature map becomes more focusing on the target segmentation objects. As for the feature map histogram, we can quantitatively discovery that the histogram peak move towards small value. We owe this observation to the fact that the Spatial Attention enhances good features and suppresses noises from trunk features.

Conv-LSTM for k-shot learning. We mainly contrast two loss variants in Conv-LSTM. (1). *1-loss Conv-LSTM*. Only output from the last shot is supervised. (2). *5-loss Conv-LSTM*. Every output from Conv-LSTM is supervised. As indicated in Table 6, the Conv-LSTM highly boosts our mIOU both in 1-shot and 5-shot learning. 1-shot result on 1-loss Conv-LSTM is 0.7% lower than our baseline, we speculate that 1-loss Conv-LSTM fails to fully supervise single-shot learning. Interestingly, both the 1-shot and 5-shot result

Table 5: Ablation Study for Attention Mechanism. ChannelAttention means SENet Block, SpatialAttention means Residual Attention Block. "sep" denotes the support branch and the query branch adopt separate attention. "share" represents the support branch and the query branch share the same attention.

Method	1-shot	#params(M)
MCG	63.3	87.2
MCG-ChannelAttention-sep[1]	63.6	89.6
MCG-ChannelAttention-share[2]	61.7	89.8
MCG-SpatialAttention-sep	63.3	93.3
MCG-SpatialAttention-share	65.8	89.5

[1] For fair comparison with SpatialAttention method, we change the fusion width to 428 to make #param nearly the same.

[2] For fair comparison with SpatialAttention method, we change the fusion width to 480 to make #param nearly the same.

Table 6: Ablation Study for loss function in Conv-LSTM. Baseline is our A-MCG module, we mainly compare the difference between 1-loss Conv-LSTM and 5-loss LSTM. The experiment is conducted on PASCAL-i^5 sub-dataset 0.

Method	1-shot	5-shot	#params(M)
baseline	65.8	66.2	89.5
1-loss Conv-LSTM	65.1	67.5	90.8
5-loss Conv-LSTM	66.1	67.9	90.8

on 5-loss LSTM outperform our baseline, which sufficiently validates our motivation.

Furthermore, we also conduct k-shot learning where k ranges from 1 to 10 in Fig. 6. k-loss Conv-LSTM fully surpasses the traditional logical or method in all shot number range. When $k \leq 4$, the performance of 1-loss Conv-LSTM is less than 5-loss Conv-LSTM, while partially larger than our baseline. This proves that our 5-loss Conv-LSTM better integrates multi-shot support features than traditional method.

Result in PASCAL VOC. As shown in Table 8, our A-MCG architecture could outperform nearly 61.2% in 1-shot mIoU, 62.2% in 5-shot mIoU. Based on our baseline, we continue applying the MCG, attention mechanism, Conv-LSTM, reach a new state-of-the-art result on PASCAL-i^5 dataset in the end.

Result in COCO Dataset. To evaluate our algorithm in more complex dataset, we evaluate our algorithm in COCO dataset. For the COCO dataset evaluation, we divide the 80 classes into 4 sub-dataset, thus every sub-dataset is comprised of 20 classes. We cross-validate the performance of our algorithm and the result is shown in Table 7. As COCO dataset owns much more classes compared with Pascal VOC (80 vs 20). The complexity of this dataset makes our performance much less obvious in COCO than in PASCAL VOC. However, the result in Table 7 demonstrates that our A-MCG-Conv-LSTM model persistently improve our base-
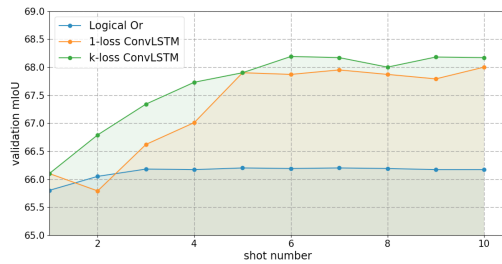

Figure 6: The relationship between shot number and validation mIoU, we mainly compare among three multi-shot learning fusion strategies: (1). Logical Or. (2). 1-loss Conv-LSTM. (3). k-loss Conv-LSTM(k=5 in our experiment). The experiment is conducted on PASCAL-i^5 sub-dataset 0.

Table 7: COCO Dataset result.

method	1-shot	5-shot	#params(M)
Baseline	49.98	51.2	85.1
A-MCG-Conv-LSTM	52	54.7	90.8

line about 3% mIoU both in 1-shot and 5-shot result.

Conclusion

We propose an Attention-based Multi-Context Guiding network (A-MCG) which incorporates multi-level concentrated context. The benefits of our network are three folds: (1). The shallow part of our network generates low-level semantic features, meanwhile deep part of our network captures high-level semantic features. Context features in equal level are fused by our MCG module, which highly facilitates the support branch to globally "support" the query branch. (2). Spatial Attention is employed along with the whole MCG branch, which makes our network focus on different scales of context information. (3). The import of Conv-LSTM enables the network to better integrate the feature from the support set in multi-shot semantic segmentation. The performance of our model surpasses state-of-the-art in few-shot semantic segmentation. In the future, we will exploit few-shot learning in multi-class segmentation at one time.

Table 8: Result on PASCAL-i^5 Dataset. All results are computed by taking the average of the 5 sub-datasets in PASCAL-i^5. The 5-shot result is obtained by logic or fusion except the method with Conv-LSTM.

Method	1-shot	5-shot	#params(M)
OSLSM (Shaban et al. 2017)	40.8	43.9	276.7
co-FCN(Multi-class) (Rakelly et al. 2018)	50.9	50.9	–
co-FCN(Overall) (Rakelly et al. 2018)	60.1	60.8	–
Baseline	53.0	54.8	85.1
MCG	55.3	56.5	87.2
A-MCG	57.3	57.8	89.5
A-MCG-Conv-LSTM	**61.2**	**62.2**	90.8

Acknowledgements

References

Abadi, M.; Barham, P.; Chen, J.; Chen, Z.; Davis, A.; Dean, J.; Devin, M.; Ghemawat, S.; Irving, G.; Isard, M.; et al. 2016. Tensorflow: A system for large-scale machine learning. In *OSDI*.

Ba, J. L.; Kiros, J. R.; and Hinton, G. E. 2016. Layer normalization. *arXiv preprint arXiv:1607.06450*.

Bottou, L. 2010. Large-scale machine learning with stochastic gradient descent. In *Proceedings of COMPSTAT'2010*.

Caelles, S.; Maninis, K.-K.; Pont-Tuset, J.; Leal-Taixé, L.; Cremers, D.; and Van Gool, L. 2017. One-shot video object segmentation. In *IEEE Conference on Computer Vision and Pattern Recognition*.

Chen, L.-C.; Papandreou, G.; Kokkinos, I.; Murphy, K.; and Yuille, A. L. 2018. Deeplab: Semantic image segmentation with deep convolutional nets, atrous convolution, and fully connected crfs. *IEEE Transactions on Pattern Analysis and Machine Intelligence*.

Deng, J.; Dong, W.; Socher, R.; Li, L.-J.; Li, K.; and Fei-Fei, L. 2009. Imagenet: A large-scale hierarchical image database. In *IEEE Conference on Computer Vision and Pattern Recognition*.

Everingham, M.; Van Gool, L.; Williams, C. K.; Winn, J.; and Zisserman, A. The pascal visual object classes (voc) challenge. *International Journal of Computer Vision*.

Gers, F. A.; Schraudolph, N. N.; and Schmidhuber, J. 2002. Learning precise timing with lstm recurrent networks. *Journal of Machine Learning Research*.

Glorot, X., and Bengio, Y. 2010. Understanding the difficulty of training deep feedforward neural networks. In *International Conference on Artificial Intelligence and Statistics*.

Hariharan, B.; Arbeláez, P.; Girshick, R.; and Malik, J. Simultaneous detection and segmentation. In *European Conference on Computer Vision*.

He, K.; Zhang, X.; Ren, S.; and Sun, J. 2016. Deep residual learning for image recognition. In *IEEE Conference on Computer Vision and Pattern Recognition*.

Hochreiter, S., and Schmidhuber, J. Long short-term memory. *Neural Computation*.

Hu, J.; Shen, L.; and Sun, G. 2018. Squeeze-and-excitation networks. *IEEE Conference on Computer Vision and Pattern Recognition*.

Ioffe, S., and Szegedy, C. 2015. Batch normalization: Accelerating deep network training by reducing internal covariate shift. In *International Conference on Machine Learning*.

Krizhevsky, A.; Sutskever, I.; and Hinton, G. E. 2012. Imagenet classification with deep convolutional neural networks. In *Advances in Neural Information Processing Systems*.

Long, J.; Shelhamer, E.; and Darrell, T. 2015. Fully convolutional networks for semantic segmentation. In *IEEE Conference on Computer Vision and Pattern Recognition*.

Nair, V., and Hinton, G. E. 2010. Rectified linear units improve restricted boltzmann machines. In *International Conference on Machine Learning*.

Newell, A.; Yang, K.; and Deng, J. Stacked hourglass networks for human pose estimation. In *European Conference on Computer Vision*.

Rakelly, K.; Shelhamer, E.; Darrell, T.; Efros, A.; and Levine, S. 2018. Conditional networks for few-shot semantic segmentation. In *International Conference on Learning Representations Workshop Papers*.

Ravi, S., and Larochelle, H. 2017. Optimization as a model for few-shot learning. In *International Conference on Learning Representations*.

Shaban, A.; Bansal, S.; Liu, Z.; Essa, I.; and Boots, B. 2017. One-shot learning for semantic segmentation. In *British Machine Vision Conference*.

Simonyan, K., and Zisserman, A. 2014. Very deep convolutional networks for large-scale image recognition. *CoRR*.

Snell, J.; Swersky, K.; and Zemel, R. 2017. Prototypical networks for few-shot learning. In *Advances in Neural Information Processing Systems*.

Szegedy, C.; Liu, W.; Jia, Y.; Sermanet, P.; Reed, S.; Anguelov, D.; Erhan, D.; Vanhoucke, V.; Rabinovich, A.; et al. 2015. Going deeper with convolutions. In *IEEE Conference on Computer Vision and Pattern Recognition*.

Vinyals, O.; Blundell, C.; Lillicrap, T.; Wierstra, D.; et al. 2016. Matching networks for one shot learning. In *Advances in Neural Information Processing Systems*.

Wang, F.; Jiang, M.; Qian, C.; Yang, S.; Li, C.; Zhang, H.; Wang, X.; and Tang, X. 2017. Residual attention network for image classification. In *IEEE Conference on Computer Vision and Pattern Recognition*.

Wu, Y., et al. 2016. Tensorpack. `https://github.com/tensorpack/`.

Xingjian, S.; Chen, Z.; Wang, H.; Yeung, D.-Y.; Wong, W.-K.; and Woo, W.-c. 2015. Convolutional lstm network: A machine learning approach for precipitation nowcasting. In *Advances in Neural Information Processing Systems*.